Microporous Materials

DOI: 10.1002/anie.201410612

Turn-On Luminescence Sensing and Real-Time Detection of Traces of Water in Organic Solvents by a Flexible Metal–Organic Framework**

Antigoni Douvali, Athanassios C. Tsipis, Svetlana V. Eliseeva, Stéphane Petoud, Giannis S. Papaefstathiou, Christos D. Malliakas, Ioannis Papadas, Gerasimos S. Armatas, Irene Margiolaki, Mercouri G. Kanatzidis, Theodore Lazarides, and Manolis J. Manos**

Abstract: *The development of efficient sensors for the determination of the water content in organic solvents is highly desirable for a number of chemical industries. Presented herein is a Mg^{2+} metal–organic framework (MOF), which exhibits the remarkable capability to rapidly detect traces of water (0.05–5 % v/v) in various organic solvents through an unusual turn-on luminescence sensing mechanism. The extraordinary sensitivity and fast response of this MOF for water, and its reusability make it one of the most powerful water sensors known.*

A simple, fast, and reliable chemical analysis method for the water content of organic solvents is essential not only for chemical industries producing dry solvents and moisture-sensitive chemicals but also for industries manufacturing oils and petroleum products, in which water is a common contaminant and impurity. In addition, the accurate determination of water content in ethanol is of high importance for the fuel, alcoholic beverage, and solvent industries.[1] Luminescent water sensors have attracted great interest because of their significant advantages over electrochemical sensors involving their capability for remote and in situ monitoring as well as the ease of their fabrication.[1,2] Undoubtedly, luminescence-based determination of the water content is a much simpler method than the traditional Karl Fischer titration which requires specialized instruments, well-trained personnel, etc.[3] So far, luminescent water sensors are limited to organic fluorescent molecules. However, the majority of such sensors are unable to detect water in very low concentrations (< 1 % v/v) and the organic fluorescent molecules cannot be readily recovered and reused.[2] In addition, the solution-phase sensing by organic molecular sensors generates liquid waste (i.e., the solution of the organic sensor).

In this context, luminescent metal–organic framework (MOF) compounds which combine inherent porosity and guest-binding ability are rather promising for sensing applications. These materials are easy to prepare and offer a green solid-state sensing process, with the capability for facile recovery and regeneration of the sensor.[4] So far, some luminescent MOFs have been tested as humidity sensors,[5] but to the best of our knowledge no studies for the use of such materials for the detection of water in organic solvents have been reported.

Herein we present the MOF $[Mg(H_2dhtp)(H_2O)_2]\cdot DMAc$, denoted AEMOF-1·DMAc (AEMOF-1 = alkaline earth MOF-1; H_4dhtp = 2,5-dihydroxy-terepthalic acid; DMAc = *N,N*-dimethylacetamide). It displays a three-dimensional (3D) open framework structure (Figure 1) with significant breathing capability as proven by the facile removal/re-adsorption of the guest DMAc molecules. Remarkably, we

[*] A. Douvali, Dr. A. C. Tsipis, Dr. M. J. Manos
Department of Chemistry, University of Ioannina
45110 Ioannina (Greece)
E-mail: emanos@cc.uoi.gr
Dr. S. V. Eliseeva, Prof. S. Petoud
Center of Molecular Biophysics, CNRS UPR 4301
Orleans (France)
Dr. G. S. Papaefstathiou
Department of Chemistry, National and Kapodistrian University of Athens, 15771 Zografou (Greece)
Dr. C. D. Malliakas, Prof. M. G. Kanatzidis
Department of Chemistry, Northwestern University
Evanston, IL 60208 (USA)
Dr. I. Papadas, Dr. G. S. Armatas
Department of Materials Science and Technology
University of Crete, 71003 Heraklion (Greece)
Dr. I. Margiolaki
Department of Biology
University of Patras, 26500 Patras (Greece)
Dr. T. Lazarides
Department of Chemistry, Aristotle University of Thessaloniki,
54124 Thessaloniki (Greece)
E-mail: tlazarides@chem.auth.gr

[**] Financial support from the National Science Foundation (Grant DMR-1410169) (MGK) and La Ligue Contre le Cancer, La Région Centre and the Institut National de la Santé et de la Recherche Médicale (SVE, SP) are gratefully acknowledged. The work in Center of Molecular Biophysics, France was carried out in the framework of European Cooperation in Science and Technology Actions TD1004 and CM1006. The variable-temperature diffraction measurements were carried out in the J. B. Cohen X-Ray Diffraction Facility supported by the MRSEC program of the National Science Foundation (DMR-1121262) at the Materials Research Center of Northwestern University. We would like also to thank the ESRF for provision of beam time at the ID22 beamline and Panalytical for the provision of the Xβ Pert Pro Lab diffractometer as well as F. Karavassili and Dr. A. Fitch for data collection at ID22 beamline. The National Strategic Reference Framework, Regional Operational Program of Epirus 2007-2013 (2011/S 29-048013), is acknowledged for supporting the purchase of an LS55 fluorimeter by the Department of Chemistry of the University of Ioannina.

Supporting information for this article is available on the WWW under http://dx.doi.org/10.1002/anie.201410612.

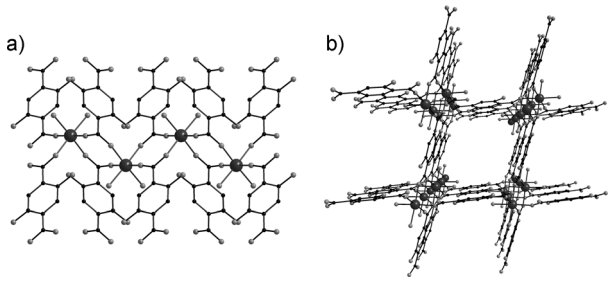

Figure 1. a) A chain of MgO_6 octahedra and b) the 3D structure of AEMOF-1. Mg dark gray, O light gray, C black. Guests (DMAc molecules) and H atoms were omitted for clarity.

find that the guest-free MOF (AEMOF-1′) is capable of water detection through an unusual luminescence turn-on sensing mechanism. Trace water concentrations (0.05–5 % v/v) in various organic solvents are detectable and in fact, the present MOF is the first example showing such sensing capability. The exceptional sensitivity and very fast response of AEMOF-1′ for water, and its reusability make it a powerful luminescent sensor for the detection/determination of water in organic solvents.

AEMOF-1·DMAc forms platelike crystals by a reaction of $Mg(OAc)_2{\cdot}4H_2O$ and H_4dhtp in DMAc/H_2O (9:1 v/v) at 120 °C. It crystallizes in the monoclinic space group *C*2/*c*[6] and features one crystallographically unique Mg^{2+}, which adopts octahedral coordination geometry and is linked with four carboxylate oxygen atoms from the H_2dhtp^{2-} ligands and two terminal water ligands. Each Mg atom is connected to two neighboring Mg atoms by four $\eta^1{:}\eta^1{:}\mu_2$-COO^-, thus forming a chain (rod) of linked MgO_6 octahedra running parallel to the *c* axis (Figure 1 a). The chains are interconnected through the H_2dhtp^{2-} linkers to form a 3D framework (Figure 1 b) which displays a solvent-accessible volume of about 45 % and size of pores approximately 6 Å, calculated by PLATON[7] (after excluding all guest DMAc solvents from the pores). Topologically the structure of AEMOF-1·DMAc can be treated as a network with twisted ladders as secondary building units (SBUs). Specifically, the carboxylate carbon atoms around the linked MgO_6 octahedra (rod SBU) form a twisted ladder (see Figure S1 in the Supporting Information). The ladders are further connected by the phenyl groups of the H_2dhtp^{2-} ligands, thus resulting in a uninodal four-coordinated network with the three-letter code irl and point symbol $4^2.6^3.8$ (Figure S1).[8] Besides crystallography, AEMOF-1·DMAc was characterized by a variety of other techniques including PXRD and thermal analysis (see Figures S2 and S3).

The fact that AEMOF-1·DMAc has a 3D structure with relatively large channels hosting highly disordered guest (DMAc) molecules (see Figure S4), motivated us to investigate the possibility of evacuating its pores with preservation of its porosity, thus activating it. The activation/evacuation of the pores of this MOF is the key feature for its unique sensor properties. Thermal treatment of the MOF seems not to be an appropriate method for its activation, since variable-temperature powder X-ray diffraction (PXRD) data indicate that the material partially decomposes upon heating at temperatures higher than 130 °C (see Figure S5). Thus, a more benign method of activation was chosen: AEMOF-1·DMAc was initially treated with MeOH to yield a MeOH-exchanged material, which was then subjected to gentle heating at 50 °C under vacuum to yield the guest-free product (AEMOF-1′). The disappearance of characteristic IR absorption peaks of DMAc in the infrared spectrum of AEMOF-1′ together with elemental, ^{1}H NMR, and thermal analyses data confirmed the removal of the guest solvent molecules (see Figures S6, S7, and S8). Powder X-ray diffraction (PXRD) data (see Figure S9) show that AEMOF-1′ is highly crystalline but its structure is significantly contracted compared to that of the as-prepared compound. The small BET surface area ($11\ m^2 g^{-1}$) of AEMOF-1′ further confirms the contraction of the structure of the MOF upon removal of the guest solvents (for BET surface area measurements, see Figures S10–S13). Remarkably, by immersing AEMOF-1′ in DMAc for a few minutes, the expanded structure of the pristine AEMOF-1·DMAc is fully restored as indicated by PXRD (Figure S9), thus revealing a significant breathing behavior and flexibility for this MOF.[9] ^{1}H NMR data of AEMOF-1′, after its treatment with THF or CH_3CN and subsequent drying in air, shows that these solvents are not retained as guests in the structure of the MOF and thus, interact very weakly with the framework. However, AEMOF-1′ can absorb about 2–4 EtOH molecules per formula unit, as indicated by ^{1}H NMR data. EtOH also evaporates from the pores of the MOF (as ^{1}H NMR data revealed), although at much slower rate (after exposure to air for 3–4 weeks) than THF or CH_3CN. Interestingly, AEMOF-1′ shows selectivity for water over THF, CH_3CN, or EtOH. Specifically, AEMOF-1′ treated with water (5 % v/v in THF, CH_3CN, or EtOH) absorbs about 6 H_2O molecules per formula unit of the MOF, as indicated by elemental analysis and TGA (Figure S8). The hydrated compound is highly crystalline, but not isostructural with the pristine MOF (for PXRD data and cell indexing of AEMOF-1·6H_2O, see Figure S14).

Interestingly, AEMOF-1 shows luminescence characteristics which are highly dependent upon its form (Figure 2). When illuminated with a laboratory UV lamp ($\lambda_{exc} \approx 360$ nm), the as prepared MOF (AEMOF-1·DMAc) shows a relatively intense turquoise fluorescence with a quantum yield of $\Phi_F = 13.1(1)\,\%$ (Figure 2 and Figure S15 A), while the guest-free compound (AEMOF-1′) shows a strongly quenched [$\Phi_F = 1.89(1)\,\%$] yellowish emission (Figure S15 B,D). The hydrated

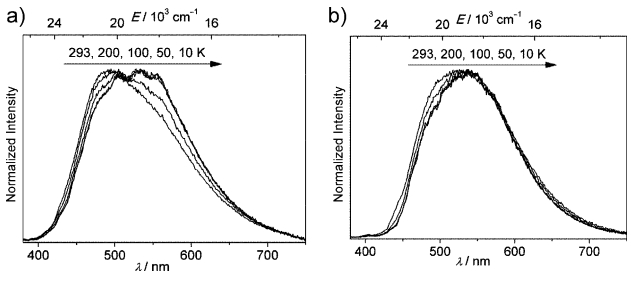

Figure 2. Solid-state fluorescence spectra ($\lambda_{exc} = 350$ nm) of the as prepared (a) and hydrated (b) forms of AEMOF-1 showing the red shift of fluorescence maxima upon lowering the temperature.

MOF (AEMOF-1·6H_2O) shows enhanced [$\Phi_F = 12.6(1)\,\%$] yellow-green fluorescence (Figures 2 and S15C). The EtOH-containing MOF (AEMOF-1·*x*EtOH) exhibits a moderate [$\Phi_F = 8.6(1)\,\%$] green emission (see Figure S16). The excitation spectra of AEMOF-1·DMAc, AEMOF-1′, AEMOF-1·*x*EtOH, and AEMOF-1·6H_2O, monitored at $\lambda = 500$ nm, are dominated by a broad absorption feature with maxima at about $\lambda = 260$ and 370 nm which is attributed to the singlet π–π* excited states of the H_2dhtp^{2-} bridging ligand (see Figure S17). The good match between the excitation and the solid-state diffuse reflectance spectra (Figure S17) demonstrates that the luminescence of the different forms of AEMOF-1 originates from the Frank-Condon first singlet excited state of the bridging ligand. In the following, we describe the luminescence properties of these four derivatives of AEMOF-1.

The fluorescence spectrum of AEMOF-1·DMAc at room temperature exhibits a broad band with maximum at about $\lambda = 493$ nm and a shoulder on its low-energy side (ca. $\lambda =$ 540 nm). Gradually lowering the temperature from 293 to 10 K, results in enhancement of the low-energy component with concomitant decline of the high-energy component of its fluorescence spectrum (Figure 2). At 10 K, it exhibits a broad-band emission with maximum at about $\lambda = 532$ nm. The possibility of significant structural modification of the material upon lowering the temperature is excluded since the single-crystal X-ray structural data of AEMOF-1·DMAc obtained at 293 and 100 K are nearly identical.[6]

In contrast, the spectrum of AEMOF-1′ consisting of a broad emission band at approximately $\lambda = 530$ nm with a shoulder at about $\lambda = 610$ nm exhibits irregular dependence on the temperature (Figure S15). The quite weak luminescence of AEMOF-1′ is likely due to the self-quenching of the emission of H_2dhtp^{2-} ligands which are in close proximity as AEMOF-1′ exhibits a relatively dense structure (BET surface area = 11 $m^2 g^{-1}$). The above explanation is supported by the observed fluorescence of AEMOF-1″, a relatively porous version of AEMOF-1 (BET surface area = 34 and 54 $m^2 g^{-1}$ calculated from N_2 and CO_2 sorption isotherms respectively, Figures S10–12; PXRD data are given in Figure S13). This material, which was activated by applying supercritical CO_2 drying on EtOH-exchanged AEMOF-1,[10] exhibits intense turquoise fluorescence upon illumination with a standard laboratory UV lamp ($\lambda = 360$ nm). Presumably, the $H_2dhtp^{2-}\cdots H_2dhtp^{2-}$ separations in AEMOF-1″ exceed the critical radius for coulombic energy transfer, thereby favoring the radiative deactivation of ligand-based excited states, whereas in the case of AEMOF-1′ the shorter interligand distances promote self-quenching of H_2dhtp^{2-} emission (Figure 3).

In contrast, AEMOF-1·6H_2O displays at room temperature a broad and largely featureless emission peak with maximum at about $\lambda = 526$ nm. This peak shows a relatively modest red-shift to approximately $\lambda = 536$ nm upon lowering the temperature to 10 K (Figure 2). AEMOF-1·*x*EtOH displays, at room temperature, a fluorescence peak with a maximum at about $\lambda = 520$ nm and a shoulder on its low-energy side (ca. $\lambda = 610$ nm), which becomes significantly more pronounced upon lowering the temperature (Figure S16). In addition, luminescence data obtained for AEMOF-1′ suspended in various solvents (THF, MeOH, EtOH, CH_3CN) demonstrate strong dependence on the nature of the solvent (Figure S18). In general it is observed that protic solvents result in red-shifted emission.

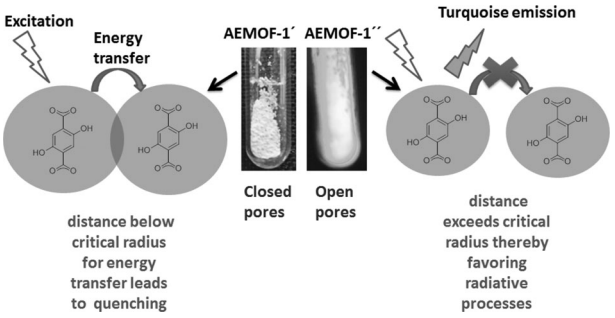

Figure 3. Self-quenching of the emission of AEMOF-1′ and the intense turquoise fluorescence of AEMOF-1″.

The above observations, especially the weak fluorescence of the guest-free MOF (AEMOF-1′) and the strong and red-shifted emission of the hydrated MOF, prompted us to test the performance of AEMOF-1′ as a luminescent sensor of moisture in organic solvents. As an example, the addition of aliquots of water into a suspension of AEMOF-1′ in dry THF results in an overall enhancement of fluorescence intensity with a concomitant red-shift of the fluorescence maximum from about $\lambda = 455$ to 530 nm (Figure 4). Note that all measurements were performed 1–2 minutes after adding the water aliquots in THF, thus indicating that AEMOF-1′ displays very fast response and capability for real-time detection of water in organic solvents. Remarkably, a considerable change in the emission profile of AEMOF-1′ is seen at a water concentration as low as 0.05 % v/v.

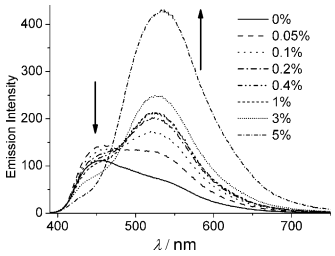

Figure 4. Changes in the fluorescence spectrum of a stirred suspension of AEMOF-1′ in dry THF upon addition of aliquots of water (0.05–5 % v/v). The excitation wavelength was $\lambda = 350$ nm.

Initially, when AEMOF-1′ is suspended in pure THF its fluorescence is significantly blue-shifted in comparison to that of the solid guest-free form (Figure 4 and Figure S15). This shift indicates that AEMOF-1′ absorbs THF under these saturated conditions. When the water content in THF reaches 5 % v/v, the suspended AEMOF-1′ displays an emission spectrum which resembles that of its hydrated form. We therefore propose that initially, in dry THF, the pores of AEMOF-1′ are filled with the organic solvent and as water is added to the system it displaces the THF molecules even-

tually leading to the formation of a hydrated form of the MOF. The fact that a very small amount of water produces a measurable change in the emission spectrum of AEMOF-1′ suggests that the latter has much greater affinity for the pores of the MOF than THF, most likely because of its ability to form strong hydrogen bonds. The weak interactions of the MOF with THF molecules were also demonstrated by the fact that THF readily evaporates from the MOF's pores when a THF-treated sample of AEMOF-1′ is left to dry in air (see above). Emission spectra of a solution of the free ligand H_4dhtp in THF in the presence of different concentrations of water are consistent with the above interpretation (Figure S19). Addition of water in THF causes a gradual red-shift in the fluorescence of H_4dhtp. However, in contrast to AEMOF-1′, a significant change in the emission profile of H_4dhtp is seen only at water concentrations above 1 % v/v. We believe that AEMOF-1′ shows higher sensitivity for water than the free H_4dhtp ligand because it has a strong tendency to absorb water and therefore increases the local concentration in its pores significantly above that in solution. In this way, the effect of water on the emission properties of the bridging ligand is greatly amplified. One more advantage of AEMOF-1′ as a moisture sensor in THF is that it shows two types of signal transduction upon analyte (water) uptake: 1) an overall enhancement of luminescence and 2) a shift in the emission maximum. Thus AEMOF-1′ offers two means of analyte detection thereby increasing specificity and eliminating possible sources of misinterpretations.[4a]

AEMOF-1′ was also tested as a moisture sensor in ethanol and acetonitrile (Figure 5 and Figure S20, respectively). In both solvents addition of water results in significant enhancement of the fluorescence of the MOF, thus indicating that

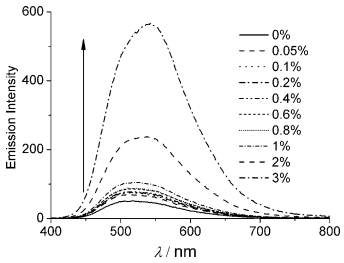

Figure 5. Changes in the fluorescence spectrum of a stirred suspension of AEMOF-1′ in dry EtOH upon addition of aliquots of water (0.05–3 % v/v). The excitation wavelength was $\lambda = 350$ nm.

AEMOF-1′ is capable of detecting water in a variety of organic solvents. It is worth noting that the observed changes in the luminescence of AEMOF-1′ are not so pronounced upon addition of extremely small quantities of water (< 1 % v/v) in EtOH. This observation may be attributed to the ability of EtOH to form relatively strong hydrogen bonds, because of its protic nature, with the free -OH groups of the framework thereby making its replacement by water molecules less facile. Nevertheless, the MOF is still more efficient in detecting water in EtOH in comparison to the free H_4dhtp ligand, as indicated by comparative luminescence experiments with the ligand in mixtures of EtOH/H_2O (see Figure S21).

To test the reusability of the sensor, a sample of hydrated MOF was treated with MeOH, dried under vacuum at 50 °C, and then immersed into DMAc to obtain a material with a fluorescence spectrum similar to that of AEMOF-1·DMAc (see Figure S22). PXRD data (see Figure S23) confirmed that the regenerated MOF is identical to the pristine material. The above tests reveal that the sensor may be recovered and reused thus offering a significant advantage over molecular (solution phase) sensors.

The fluorescence properties of the different forms of AEMOF-1 can be explained on the basis of the excited-state intramolecular proton transfer (ESIPT) which occurs in the H_2dhtp^{2-} bridging ligand upon excitation.[2d,f,11] To this end, we calculated the potential energy surfaces (PESs) of the ground state (S_0) and the lowest-energy excited singlet state (S_1) of the H_2dhtp^{2-} bridging ligand along the proton-transfer coordinate in the gas phase and aqueous solution (computational details and detailed discussion of the results are given in the Supporting Information). The computed PESs along with the calculated excitation and emission transitions are shown in Figure 8, while the structures located on the PESs are given in Figures 6 and 7.

The results confirmed the existence of dual emission from closely spaced excited states. The high-energy component is attributed to the HOMO←LUMO + 1 transition ($A_{gas} \leftarrow A_{gas}^*$ in gas phase and $A_{aq} \leftarrow A_{aq}^*$ in aqueous solution; Figure 8) with HOMO and LUMO + 1 being inherently the π and π*, respectively, MOs) of the H_2dhtp^{2-} bridging ligand delocalized mainly on the six-membered carbocyclic ring (see Figure S24). The low-energy component arises from the de-excitation of the lowest-energy fluorophore structure located on the ESIPT PES and is assigned also as an intraligand π←π* transition ($C_{gas} \leftarrow C_{gas}^*$ in gas phase, $B_{aq} \leftarrow B_{aq}^*$ in aqueous solution; Figure 8). The lowest energy ESIPT structure is more stabilized in aqueous solution (B_{aq}^*, 15.4 kcal mol^{-1}) than in gas phase (C_{gas}^*, 15.9 kcal mol^{-1}). Dual emission from closely spaced excited states, possibly in

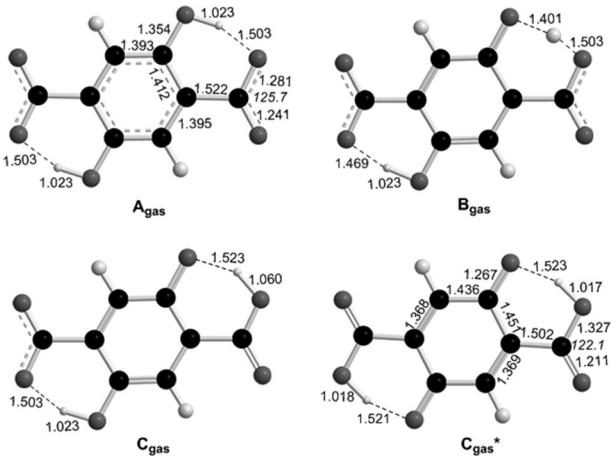

Figure 6. Selected structural parameters of minimum energy structures of H_2dhtp^{2-} located on the PESs in gas phase (C black, O gray, H light gray). A_{gas}, B_{gas}, C_{gas}, correspond to S_0 states of fluorophore structures located on the GSIPT PES and C_{gas}* corresponds to the S_1 state of the lowest-energy fluorophore structure located on the ESIPT PES.

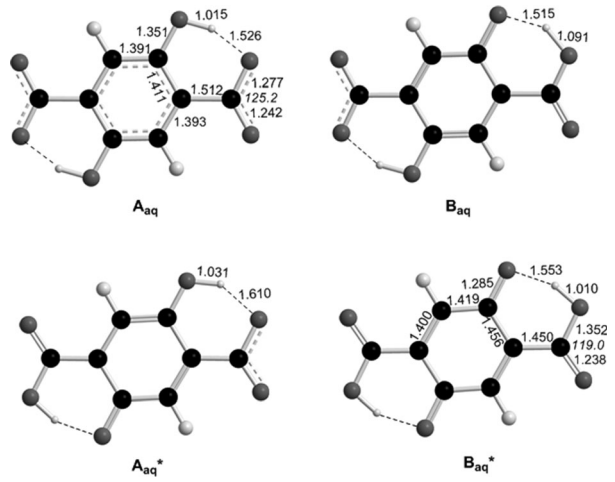

Figure 7. Selected structural parameters of minimum energy structures of H_2dhtp^{2-} located on the PESs in aqueous solution (C black, O gray, H light gray). A_{aq} and B_{aq} correspond to S_0 states of fluorophore structures located on the GSIPT PES, while A_{aq}* and B_{aq}* correspond to S_1 states of the fluorophore structures located on the ESIPT PES.

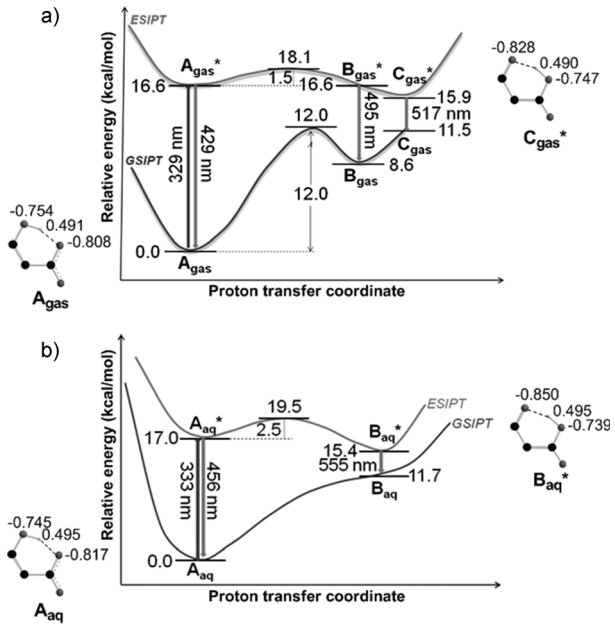

Figure 8. Potential energy surfaces of the possible photophysical processes along the proton-transfer coordinate in the gas phase (a) and in aqueous solution (b) for the H_2dhtp^{2-} ligand calculated at the PBE0/6-311++G(d,p) level of theory. A_{gas}, B_{gas}, C_{gas}, A_{aq}, B_{aq} correspond to S_0 states of fluorophore structures located on the GSIPT PES and A_{gas}*, B_{gas}*, C_{gas}*, A_{aq}*, B_{aq}* correspond to S_1 states of the fluorophore structures located on the ESIPT PES. The natural atomic charges on the O···H···O atoms of A_{gas}, A_{aq}, C_{gas}*, B_{aq}* structures are also given (O gray, H light gray).

thermal equilibrium,[12] may explain the temperature-induced change in the fluorescence properties of AEMOF-1·DMAc. Thus, at low temperatures where thermal activation of the reverse ESIPT process is not favored, the equilibrium shifts towards the lowest-energy excited state thereby leading to the observation of predominantly the low-energy component of AEMOF-1 fluorescence (Figure 1a). The stabilization of the B_{aq}* structure of H_2dhtp^{2-} in aqueous solution is consistent with the experimentally observed low-energy emission of the hydrated MOF (and in general AEMOF-1 incorporating protic solvents) and could be due to the intermolecular hydrogen-bond formation between the B_{aq}* fluorophore and the protic solvent. The redistribution of electron density occurring along the proton-transfer coordinate accumulates electron density on the O atom of the proton donor (Figure 8b) and this atom is one of the plausible electronegative centers for hydrogen-bond formation with protic solvents. Another plausible center for intermolecular hydrogen-bond formation is the transferred proton which acquires a higher positive natural atomic charge in aqueous solution than in gas phase.

In conclusion, a new Mg^{2+}-H_2dhtp^{2-} MOF (AEMOF-1·DMAc) has been isolated and features a highly flexible 3D structure with remarkable framework breathing capacity. The compound represents a rare case of an MOF with ESIPT-based luminescence and the detailed study provided here strongly contributes in the understanding of the ESIPT process in MOFs photochemistry. Remarkably, the guest-free compound (AEMOF-1′) acts as a highly efficient luminescent sensor for the detection, in real time, of traces of water in various organic solvents, a property which is relevant to important industrial applications. Interestingly, the water detection by AEMOF-1′ is achieved through a highly unusual turn-on luminescence sensing mechanism, and is in marked contrast to the common water sensing methods which are based on luminescence quenching. In fact, AEMOF-1′ is a much more effective water sensor than the H_4dhtp organic ligand and other organic molecular sensors, since the ability of AEMOF-1′ to selectively absorb water molecules and confine them in its pores in high local concentrations induces a stronger solvatochromic effect on the fluorescence of the bridging ligand. An additional advantage of AEMOF-1′ over conventional organic sensors is the regeneration capability/reusability of the MOF, as this is desirable for practical applications. Finally, a general conclusion from this work is that MOFs with ESIPT-active bridging ligands may constitute a new class of chemosensors. Our efforts are currently directed towards the further development of these materials.

Experimental Section

$Mg(OAc)_2{\cdot}4H_2O$ (0.08 g, 0.37 mmol) was added as a solid into a stirred solution of H_4dhtp (0.12 g, 0.61 mmol) in 5 mL DMAc/H_2O (9:1 v/v), in a Teflon cup. The mixture was stirred for ca. 5 min and then, the Teflon cup was transferred into a 23 mL Teflon-lined stainless steel autoclave. The autoclave was sealed and placed in an oven operated at 120 °C, remained undisturbed at this temperature for 20 h and was then cooled to room temperature. Colorless platelike crystals of AEMOF-1·DMAc were isolated by filtration and dried in the air. Yield: 0.09 g. A typical synthesis of AEMOF-1′ involves the treatment of AEMOF-1·DMAc (ca. 40 mg) with MeOH (ca. 10 mL) for 12 h, followed by drying the MeOH-exchanged material at 50 °C under vacuum for 3–4 h to afford the guest-free compound. The hydrated (AEMOF-1·6H_2O) and EtOH-exchanged (AEMOF-1·xEtOH) MOFs are typically prepared by the treatment of

AEMOF-1′ (ca. 20 mg) with water (5% v/v in ca. 2 mL of THF) and EtOH (absolute) for ca. 2 h, respectively. The details for the characterization of the materials are given in the Supporting Information.

Received: October 31, 2014
Published online: December 8, 2014

Keywords: crystal engineering · luminescence · metal–organic frameworks · microporous materials · sensors

[1] W.-E. Lee, Y.-J. Jin, L.-S. Park, G. Kwak, *Adv. Mater.* **2012**, *24*, 5604.

[2] a) Q. Deng, Y. Li, J. Wu, Y. Liu, G. Fang, S. Wang, Y. Zhang, *Chem. Commun.* **2012**, *48*, 3009; b) Y. Ooyama, K. Uenaka, A. Matsugasako, Y. Harima, J. Ohshita, *RSC Adv.* **2013**, *3*, 23255; c) Y. Ooyama, M. Sumomogi, T. Nagano, K. Kushimoto, K. Komaguchi, I. Imae, Y. Harima, *Org. Biomol. Chem.* **2011**, *9*, 1314; d) J. Wu, W. Liu, J. Ge, H. Zhang, P. Wang, *Chem. Soc. Rev.* **2011**, *40*, 3483; e) W.-H. Chen, Y. Xing, Y. Pang, *Org. Lett.* **2011**, *13*, 1362; f) H. Mishra, S. Maheshwary, H. B. Tripathi, N. Sathyamurthy, *J. Phys. Chem. A* **2005**, *109*, 2746; g) N. Suzuki, A. Fukazawa, K. Nagura, S. Saito, H. K. Nishioka, D. Yokogawa, S. Irle, S. Yamaguchi, *Angew. Chem. Int. Ed.* **2014**, *53*, 8231; *Angew. Chem.* **2014**, *126*, 8370.

[3] Y. Y. Liang, *Anal. Chem.* **1990**, *62*, 2504.

[4] a) L. E. Kreno, K. Leong, O. K. Farha, M. Allendorf, R. P. Van Duyne, J. T. Hupp, *Chem. Rev.* **2012**, *112*, 1105; b) Y. Takashima, V. M. Martínez, S. Furukawa, M. Kondo, S. Shimomura, H. Uehara, M. Nakahama, K. Sugimoto, S. Kitagawa, *Nat. Commun.* **2011**, *2*, 168; c) D. Liu, K. Lu, C. Poon, W. Lin, *Inorg. Chem.* **2014**, *53*, 1916; d) B. Chen, L. Wang, Y. Xiao, F. R. Fronczek, M. Xue, Y. Cui, G. Qian, *Angew. Chem. Int. Ed.* **2009**, *48*, 500; *Angew. Chem.* **2009**, *121*, 508; e) B. V. Harbuzaru, A. Corma, F. Rey, P. Atienzar, J. L. Jorda, H. Garcia, D. Ananias, L. D. Carlos, J. Rocha, *Angew. Chem. Int. Ed.* **2008**, *47*, 1080; *Angew. Chem.* **2008**, *120*, 1096; f) S. V. Eliseeva, J.-C. G. Bunzli, *Chem. Soc. Rev.* **2010**, *39*, 189; g) T. M. Reineke, M. Eddaoudi, M. Fehr, D. Kelley, O. M. Yaghi, *J. Am. Chem. Soc.* **1999**, *121*, 1651; h) Z. Hu, B. J. Deibert, J. Li, *Chem. Soc. Rev.* **2014**, *43*, 5815.

[5] a) Y. Yu, J.-P. Ma, Y.-B. Dong, *CrystEngComm* **2012**, *14*, 7157; b) Y. Yu, X. M. Zhang, J.-P. Ma, Q.-K. Liu, P. Wang, Y. B. Dong, *Chem. Commun.* **2014**, *50*, 1444.

[6] Single-crystal X-ray diffraction data were collected (on two different crystals) at 293 and 100 K. AEMOF-1·DMAc at 293 K: $C_{12}H_{17}MgNO_9$, $M = 343.58$, monoclinic, space group *C2/c*, $a = 13.741(3)$, $b = 13.972(3)$, $c = 8.8045(18)$ Å, $\beta = 113.76(3)°$, $V = 1547.1(7)$ Å^3, $Z = 4$, $\rho_{calcd} = 1.475$ g cm^{-3}, $T = 293(2)$ K, $2\theta_{max} = 50$, $R_{int} = 0.0260$, $R_1 = 0.0452$ ($I > 2\sigma(I)$), $wR_2 = 0.1311$ ($I > 2\sigma(I)$). AEMOF-1·DMAc at 100 K: $C_{12}H_{17}MgNO_9$, $M = 343.58$, monoclinic, space group *C2/c*, $a = 13.5104(4)$, $b = 14.1107(4)$, $c = 8.8000(3)$ Å, $\beta = 114.617(2)°$, $V = 1525.17(8)$ Å^3, $Z = 4$, $\rho_{calcd} = 1.496$ g cm^{-3}, $T = 100(2)$ K, $2\theta_{max} = 68$, $R_{int} = 0.0901$, $R_1 = 0.0646$ ($I > 2\sigma(I)$), $wR_2 = 0.2038$ ($I > 2\sigma(I)$). CCDC 1020008 and 1020009 contain the supplementary crystallographic data for this paper. These data can be obtained free of charge from the Cambridge Crystallographic Data Centre via www.ccdc.cam.ac.uk/data_request/cif.

[7] A. L. Spek, *J. Appl. Crystallogr.* **2003**, *36*, 7.

[8] a) M. O'Keeffe, O. M. Yaghi, *Chem. Rev.* **2012**, *112*, 675; b) V. A. Blatov, A. P. Shevchenko, D. M. Proserpio, *Cryst. Growth Des.* **2014**, *14*, 3576.

[9] a) G. Férey, *Chem. Soc. Rev.* **2008**, *37*, 191; b) S. Horike, S. Shimomura, S. Kitagawa, *Nat. Chem.* **2009**, *1*, 695; c) E. J. Kyprianidou, T. Lazarides, S. Kaziannis, C. Kosmidis, G. Itskos, M. J. Manos, A. J. Tasiopoulos, *J. Mater. Chem. A* **2014**, *2*, 5258; d) K. C. Stylianou, R. Heck, S. Y. Chong, J. Bacsa, J. T. A. Jones, Y. Z. Khimyak, D. Bradshaw, M. J. Rosseinsky, *J. Am. Chem. Soc.* **2010**, *132*, 4119.

[10] A. P. Nelson, O. K. Farha, K. L. Mulfort, J. T. Hupp, *J. Am. Chem. Soc.* **2009**, *131*, 458.

[11] a) N. B. Shustova, A. F. Cozzolino, S. Reineke, M. Baldo, M. Dinca, *J. Am. Chem. Soc.* **2013**, *135*, 13326; b) K. Jayaramulu, P. Kanoo, S. J. George, T. K. Maji, *Chem. Commun.* **2010**, *46*, 7906.

[12] a) K.-C. Tang, M.-J. Chang, T.-Y. Lin, H.-A. Pan, T.-C. Fang, K.-Y. Chen, W.-Y. Hung, Y.-H. Hsu, P.-T. Chou, *J. Am. Chem. Soc.* **2011**, *133*, 17738; b) C.-C. Hsieh, C.-M. Jiang, P.-T. Chou, *Acc. Chem. Res.* **2010**, *43*, 1364.

